Cherenkov radiation of electromagnetic waves by electron beams in the absence of an external magnetic field

G. S. Nusinovich
Institute for Plasma Research, University of Maryland, College Park, College Park, Maryland 20742

Yu. P. Bliokh
Kharkov Institute of Physics and Technology, 1 Akademicheskaya Street, Kharkov 310108, Ukraine

(Received 20 December 1999)

In conventional sources of coherent Cherenkov electromagnetic radiation, the electrons move linearly, guided by external magnetic fields. In the absence of such fields, the electrons can move radially, being affected by the beam self-fields as well as by the radial component of the electric field of the wave. This radial motion can, first, improve the coupling of electrons to the field of a slow wave localized near the wall of a slow-wave structure, and second, cause an energy exchange between the electrons and the wave due to an additional transverse interaction. This interaction, in particular, can lead to an experimentally observed excitation of nonsymmetric transverse electric waves in Cherenkov devices. In plasma-filled sources, the beam self-fields can be compensated for by ions, leading to a known ion focusing of the beams. In such regimes, the beam can be surrounded by an ion layer creating a potential well for electrons which can be displaced from stationary trajectories by transverse fields of the wave. The operation of such sources when the presence of ions and the radial electric field of the wave play competing focusing and defocusing roles, and electron interception by the walls restricts the output power level, is analyzed in stationary and nonstationary regimes.

PACS number(s): 41.60.Bq, 84.40.Fe, 52.75.Va, 07.57.Hm

I. INTRODUCTION

A large number of sources of coherent electromagnetic microwave radiation are based on the interaction of electrons with electromagnetic waves whose phase velocity, v_{ph}, is close to the electron velocity v_z. The radiation of such waves was first observed by Cherenkov and Vavilov in a medium with a dielectric constant $\epsilon > 1$. Later, the radiation from electrons propagating over the grating, which was first observed by Smith and Purcell [1], was also understood as a Cherenkov synchronism between electrons and a slow spatial harmonic of the wave in a periodic slow-wave structure.

Periodic (and quasiperiodic) slow-wave structures (SWS's) are used in practically all traveling-wave tubes (TWT's) and backward-wave oscillators (BWO's). Conventional TWT's and BWO's driven by low-voltage electron beams are classical microwave tubes well described in numerous textbooks; see, e.g., Refs. [2] and [3]. Among high-power microwave sources driven by relativistic electron beams, BWO's were the first devices in which efficient operation (with efficiency above 10%) was demonstrated [4,5]. Later, the efficiency of relativistic BWO's was increased to 30–40 % [6,7], and relativistic TWT's with up to 55% efficiency were developed [8]. In all these sources of coherent electromagnetic radiation, linear electron beams are used. These beams are usually guided by external magnetic fields produced by either heavy and bulky solenoids or permanent magnets.

Recently, an attempt was made to avoid the use of external magnetic fields for guiding intense electron beams. Instead, it was suggested [9] that the beam transport be provided by adding some plasma, which leads to ion focusing of the beam electrons, a process known as the Benneth pinch [10]. As a result, a number of PASOTRON's (the acronym for plasma-assisted slow-wave oscillator) were developed which utilized various slow-wave structures and operated either as backward-wave oscillators or as forward-wave amplifiers [11,12].

The performance of PASOTRON oscillators and amplifiers not only demonstrated the possibility of generating high-power electromagnetic (EM) radiation in the absence of guiding magnetic fields, but also clearly showed that the radial motion of electrons can be important for the operation of these devices. In particular, this can be the only explanation for the excitation of transverse-electric waves observed in experiments [11], since such waves cannot be excited by linear electron beams.

This motion may yield both positive and negative effects. Among the positive effects is an increase in the coupling impedance of electrons moving outward to the wave localized near the SWS walls. This effect can be especially important for BWOs, in which the wave amplitude is large near the beam entrance and small near the well-matched exit. Such an axial profile is unfavorable for the efficiency because electrons are modulated by a strong field and decelerated in a weak field. Clearly, the radial displacement in such a case increases the Lorentz force, decelerating electron bunches near the exit, and thus increases the efficiency. Another positive effect can stem from the influence of the radial electric field of the wave upon electrons moving radially. Added in a proper phase to the electron axial deceleration, this effect may increase the interaction between the electrons and the wave. Correspondingly, the efficiency can be enhanced, and the interaction region can be shortened.

The most deleterious effect is electron bombardment of SWS walls, which may cause rf breakdown, leading to microwave pulse shortening. The latter issue seems to be one of the most crucial for the development of high-power micro-

wave sources [13,14]. (Note that here, we are not discussing such obvious effects as the deterioration of a SWS surface by the beam.)

In this paper, we make an attempt to analyze the sources of high-power Cherenkov EM radiation driven by relativistic electron beams in the absence of a guiding magnetic field. The paper is organized as follows. In Sec. II we consider some restrictions on the power level and the choice of parameters in such devices. In Sec. III we present equations describing the interaction between electrons and slow EM waves in the absence of guiding magnetic field and self-fields of the beam. In Sec. IV we present the results of the small-signal analysis and large-signal simulations of these equations. In Sec. V we discuss the creation of ions by the electron beam, and consider the effects of ions and beam self-fields on the performance of devices. Finally, Sec. VI contains a discussion of the results obtained and the conclusions.

II. LIMITATIONS ON RADIATED POWER AND CHOICE OF PARAMETERS

In this section, we will estimate the maximum level of radiated power allowed by rf breakdown and the parameters of the SWS that make efficient operation of a Cherenkov radiation source possible in the absence of an external magnetic field.

A. Maximum radiated power

Let us consider a periodic rippled-wall, finite-length SWS in which an initially linear electron beam can excite one of symmetric transverse-magnetic waves. Nonzero components of the wave fields of such a structure in the absence of beam self-fields can be determined as

$$E_z=\mathrm{Re}\left\{e^{-i\omega t}\sum_n\ ia_n\frac{g_n}{\omega/c}J_0(g_nr)e^{ik_{zn}z}\right\},$$

$$E_r=\mathrm{Re}\left\{e^{-i\omega t}\sum_n\ a_n\frac{k_{zn}}{\omega/c}J_1(g_nr)e^{ik_{zn}z}\right\}, \qquad (1)$$

$$H_\phi=\mathrm{Re}\left\{e^{-i\omega t}\sum_n\ a_nJ_1(g_nr)e^{ik_{zn}z}\right\}.$$

Here, in accordance with Floquet's theorem, the wave is represented as the superposition of spatial harmonics with axial wave numbers, $k_{z,n}=k_{z0}+n2\pi/d$ (where d is the structure period), ω is the wave frequency, $k_{z,0}$ is the wave number of the zeroth-order harmonic $(-\pi/d<k_{z0}<\pi/d)$, g_n is the transverse wave number of the nth harmonic $[g_n^2=(\omega/c)^2-k_{z,n}^2]$, and a_n is the nth harmonic amplitude. As will be discussed below, the amplitudes of nonzero harmonics depend on the height of the ripples. At the exit from the SWS, the height of the ripples adiabatically diminishes to zero, so the radiated power can be determined as

$$P=\tfrac{1}{8}|a_0|^2ch_0R_0^2J_1^2(\nu). \qquad (2)$$

In Eq. (2), $h_0=k_{z0}/(\omega/c)$ is the dimensionless axial wave number, c the speed of light, R_0 is the waveguide radius, and ν is the mode eigennumber, which is determined by the boundary condition at the wall, $J_0(\nu)=0$ ($\nu_{01}=2.405$, $\nu_{02}=5.52$, etc.). Note that in the case of a shallow SWS, the amplitude of the zero harmonic is much larger than the amplitudes of other harmonics everywhere, so Eq. (2) can be used for the field inside such an SWS. In particular, the ratio a_1/a_0, as shown elsewhere [15,16], is linearly proportional to l/R_0, where l is the height of the ripples.

The breakdown field at the wall of a cylindrical waveguide is determined by the radial component of the electric field, $E_r(R_0)\approx a_0h_0J_1(\nu)$. So, when the maximum value for this field, $E_{r,\max}$, is known, the maximum radiated power, as follows from Eq. (2), can be determined as

$$P_{\max}\simeq 4.165|h_0|^{-1}E_{r,\max}^2R_0^2. \qquad (3)$$

In Eq. (3) $P_{\max}$, $E_{r,\max}$, and R_0 are given in GW, MV/m, and m, respectively. So, for instance, if we consider an X-band source (the wavelength $\lambda\simeq 3$ cm) operating at the TM_{01} mode with an SWS of a radius of about 2 cm and, in accordance with Ref. [17], assume $E_{r,\max}\approx 20$ MV/m, then Eq. (3) yields $P_{\max}\approx 0.8$ GW. (Note that the breakdown field depends on a number of factors discussed elsewhere [13,14,17]).

An intriguing feature of Eq. (3) is the presence of h_0 in the denominator, which indicates that a higher power can be achieved in the case of operation near cutoff. In Eq. (2), this h_0 appears, as usual, in the numerator. However, when the operation becomes closer to the cutoff, the radial electric field, as follows from Eq. (1), vanishes, and this fact alone allows a tube to withstand operation at high power levels without breakdown. [Of course, inside a SWS, an electric field normal to a rippled wall is a superposition of the radial and axial components, so accounting for E_z modifies Eq. (3).]

B. Radial displacement of electrons

To simplify our initial treatment, let us neglect the beam self-fields. Then the radial motion of electrons in the synchronous field of a TM_{op} wave can be described by the equation for the radial component of electron momentum:

$$\frac{dp_r}{dt}=ea(h-\beta_z)I_1(|g|r)\sin\theta. \qquad (4)$$

Here, a, h, and g designate corresponding values for the spatial harmonic synchronous with electrons, and $\theta=k_zz-\omega t$ is a slowly variable phase. Using the condition of Cherenkov synchronism, $v_{\mathrm{ph}}\approx v_z$, which can be rewritten as $h\approx 1/\beta_z$, and assuming that (1) the changes in electron energy and axial velocity are small enough; (2) the argument $|g|r$ in the first-order modified Bessel function is also small, so that $I_1(|g|r)\approx 1/2|g|r$; and (3) in the worst case of maximum displacement, $\sin\theta=1$, one can rewrite Eq. (4) as (cf. Ref. [18])

$$\frac{d^2r}{dt^2}=\Omega_r^2r, \qquad (5)$$

where

$$\Omega_r^2=\frac{ea}{m_0c\omega}\frac{1}{2\gamma_0^2(\gamma_0^2-1)}\omega^2.$$

Here γ_0 is the initial electron energy normalized to the rest energy. Equation (5) has an exponentially growing solution, from which it follows that electrons with an initial radial coordinate r_{b0} will not reach a SWS wall of a radius R_w when the normalized amplitude of the synchronous spatial harmonic, $A_s=ea/m_0c\omega$, and the interaction length L, obey the following restriction:

$$\left(\frac{1}{2}A_s\right)^{1/2}\frac{L}{\lambda}<\frac{\gamma_0^2-1}{2\pi}\ln(R_w/r_{b0}). \tag{6}$$

Note that, at large radii, for which the approximation of the modified Bessel function given above is incorrect, the corresponding restriction on the field amplitude and the interaction length is more stringent.

The choice of the field amplitude and the interaction length can be done based on the analysis of electron axial motion. The axial momentum of electrons can be described by

$$\frac{dp_z}{dt}=ea\kappa I_0(|g|r)\cos\theta, \tag{7}$$

where $\kappa=|g|/(\omega/c)$ is the dimensionless transverse wave number of the synchronous spatial harmonic. [In Eq. (7), we neglected the Lorentz force originating from the azimuthal magnetic field of the wave and the electron radial motion.] Combining Eq. (7) with the equation for a slowly variable phase,

$$\frac{d\theta}{dt}=k_zv_z-\omega,$$

under the same assumptions as noted above, yields a nonlinear pendulum equation

$$\frac{d^2\theta}{dt^2}=\Omega_z^2\cos\theta, \tag{8}$$

which is well known in the theory of traveling-wave tubes [19] and free electron lasers [20]. The frequency Ω_z in Eq. (8) relates to the frequency Ω_r in Eq. (5) as $\Omega_z^2=\Omega_r^2I_0(|g|r)2\gamma_0^2\simeq 2\gamma_0^2\Omega_r^2$.

So, estimating the condition of significant phase trapping as $\Omega_zT\sim\pi$ (where $T=L/v_z$ is the electron transit time), and combining this condition with Eq. (6), yields

$$\ln(R_w/r_{b0})>\frac{\pi}{\sqrt{2}\gamma_0}. \tag{9}$$

Equation (9) determines the clearance between the beam and the SWS walls required for the beam transport through the interaction region in the absence of guiding magnetic field.

Recall that in the case of BWO's the electrons interact synchronously with the minus first spatial harmonic, while the radiation power is mainly carried by the zero harmonic. In contrast, in TWTs the same slow-wave zero harmonic is responsible for both the interaction with electrons and the power flow, so for TWTs these estimates should be modified properly. Note that this consideration can be supplemented with the estimates of the synchronous field amplitude and the interaction length given in Ref. [21].

III. GENERAL FORMALISM

Let us assume that the initial spread in electron velocities is negligibly small, and that the presence of immobile ions compensates for the radial Lorentz force associated with the static self-fields of the beam. Then a self-consistent set of equations will contain equations for electron motion under the action of the wave fields given by Eq. (1) and the equation for the wave amplitude describing the wave excitation in a shallow SWS by the beam. We will also assume that the spread in electron radial coordinates at the entrance is negligibly small, which is valid for a thin annular electron beam. The latter assumption allows us to use a so-called ''hard-disk'' model of the beam. In this model, the electrons' radial displacement depends on the entrance time (i.e., the initial phase with respect to the wave), but all particles entering the interaction region at the time t_0 undergo the same displacement under the action of the wave.

In such a model, the electron momentum p, energy γ, phase θ, radial coordinate r, and wave amplitude A, after a certain normalization, can be described by the following set of equations:

$$\frac{dp_z}{dz}=\frac{\gamma}{p_z}\hat{I}_0(\rho)\kappa\,\mathrm{Re}(Ae^{i\theta})+\frac{p_r}{p_z}\hat{I}_1(\rho)\mathrm{Im}(Ae^{i\theta}), \tag{10}$$

$$\frac{dp_r}{dz}=\left(h\frac{\gamma}{p_z}-1\right)\hat{I}_1(\rho)\mathrm{Im}(Ae^{i\theta}), \tag{11}$$

$$\frac{d\gamma}{dz}=\kappa\hat{I}_0(\rho)\mathrm{Re}(Ae^{i\theta})+h\frac{p_r}{p_z}\hat{I}_1(\rho)\mathrm{Im}(Ae^{i\theta}), \tag{12}$$

$$\frac{d\theta}{dz}=\Delta+\frac{\gamma_0}{p_{z0}}-\frac{\gamma}{p_z}, \tag{13}$$

$$\frac{dr}{dz}=\frac{p_r}{p_z}, \tag{14}$$

$$\frac{\partial A}{\partial z}-\frac{1}{\beta_{gr}}\frac{\partial A}{\partial t}=-I\frac{1}{2\pi}\int_0^{2\pi}\left[\kappa\hat{I}_0(\rho)+ih\frac{p_r}{p_z}\hat{I}_1(\rho)\right]e^{-i\theta}d\theta_0. \tag{15}$$

Here β_{gr} is the wave group velocity normalized to the speed of light and in equations for electron motion:

$$\frac{d}{dz}=\frac{\partial}{\partial z}+\frac{1}{\beta_z}\frac{\partial}{\partial t}.$$

We will supplement these equations with the expression for the electron efficiency,

$$\eta=\frac{1}{\gamma_0-1}\left\{\gamma_0-\frac{1}{2\pi}\int_0^{2\pi}\gamma d\theta_0\right\}. \tag{16}$$

In Eqs. (10)–(15), the electron momentum is normalized to m_0c, and coordinates to ω/c; the modified Bessel functions

of the argument, $\rho=|g|r$, are normalized to $I_0(|g|r_{b0})$, where r_{b0} is the initial radial coordinate of electrons; the complex wave amplitude, A, is A_s, introduced above, multiplied by $I_0(|g|r_{b0})$; and the normalized beam current parameter in Eq. (15) is equal to

$$I=\frac{eI_b}{m_0c^3}2\frac{c^3}{\omega^2 N}\left|\frac{a_{-1}}{a_0}\right|^2 I_0^2(|g|r_{b0}). \tag{17}$$

Also in Eq. (13), $\Delta=(1/\beta_{z0})-(1/\beta_{ph})$ is the initial mismatch of the Cherenkov synchronism. In Eq. (17), the norm of the wave, N, is proportional to the power flow given by Eq. (2) [$P=(|a_0|^2/4)N$]; the ratio $|a_{-1}/a_0|^2$ is given for the case of a BWO (for a TWT, this ratio should be omitted). When the height of the ripples on an SWS wall is small in comparison with the wavelength, the ratio $|a_{-1}/a_0|$ can be determined by the analytical formula given in Ref. [15]:

$$\frac{a_{-1}}{a_0}=-i\frac{l}{2}\frac{J_1(g_0R_0)[g_0^2+h_0 2\pi/d]}{|g|I_0(|g|R_0)}.$$

Note that in the case of BWO's, the wave propagates toward the entrance, so the norm N is negative, and correspondingly, the sign of the normalized current parameter, I, in Eq. (15) should be changed. Also, the boundary conditions to Eq. (15) for the cases of TWTs and BWO's are different: for a TWT, $A(0)=A_0$; for a BWO with a well-matched output, $A(\zeta_{\text{out}})=0$, and in the case of a BWO with nonzero end reflections, the wave amplitude at the exit depends on the reflection coefficient (see, e.g., Ref. [22]).

In the stationary regime, Eqs. (12), (15), and (16), being properly combined, yield the energy conservation law, which in the case of a TWT can be written as

$$|A|^2-|A_0|^2=2I(\gamma_0-1)\eta. \tag{18}$$

This law can also be written in a similar form for BWO's.

For the case of stationary operation, when the changes in the electron energy and velocity are small, one can reduce Eqs. (10)–(15) to the following set of equations:

$$\frac{d^2\theta}{d\zeta^2}=\hat{I}_0(\rho)\mathrm{Re}(\alpha e^{i\theta}), \tag{19}$$

$$\frac{d^2\rho}{d\zeta^2}=\hat{I}_1(\rho)\mathrm{Im}(\alpha e^{i\theta}), \tag{20}$$

$$\frac{d\alpha}{d\zeta}=-\frac{1}{2\pi}\int_0^{2\pi}\hat{I}_0(\rho)e^{-i\theta}d\theta_0. \tag{21}$$

In reducing Eqs. (10)–(15) to Eqs. (19)–(21), we used the condition of Cherenkov synchronism for expressing κ and h via initial electron energy, introduced the Pierce gain parameter C by $C^3=I/(\gamma_0^2-1)^{5/2}$, and normalized the axial coordinate and the field amplitude to C: $\zeta=Cz$, $\alpha=A/(\gamma_0^2-1)^2C^2$. The boundary conditions to Eqs. (19) and (20) can be written as $\theta(0)=\theta_0\epsilon[0;2\pi)$, $d\theta/d\zeta|_0=\Delta'$ (where $\Delta'=\Delta/C$; the prime will be omitted hereafter), and $\rho(0)=\rho_0$, $d\rho/d\zeta|_0=0$. When the radial displacement is small, Eqs. (19) and (20) yield Eqs. (8) and (5), respectively. Note that Eqs. (19)–(21) also allow us to calculate the normalized efficiency,

$$\hat{\eta}=\Delta-\frac{1}{2\pi}\int_0^{2\pi}\frac{d\theta}{d\zeta}d\theta_0, \tag{22}$$

which, as is known in the theory of TWT's and BWO's [19,23], relates to the electron efficiency given by Eq. (16), as

$$\eta=(\gamma_0+1)\sqrt{\gamma_0^2-1}C\hat{\eta}. \tag{23}$$

IV. RESULTS

A. Small-signal theory

In the framework of the small-signal theory, the action of the EM wave on electrons can be considered as a perturbation in the electron motion. Linearizing Eqs. (10)–(15) with respect to these perturbations, and assuming that they propagate along z as $\sim\exp(i\Gamma z)$, one can readily derive the following dispersion equation:

$$\Gamma^2(\Gamma-\Delta)+\frac{C^3}{2}[1+q(1-\Gamma\beta_{z0}\gamma_0^2)]=0. \tag{24}$$

Here $q=I_1^2(\rho_0)/I_0^2(\rho_0)$ describes the ratio of beam coupling impedances to the radial and axial electric fields at the entrance. In the case of small C's, one can introduce $\gamma=2^{1/3}\Gamma/C$ and $\delta=2^{1/3}\Delta/C$, and, omitting small terms ($\sim C$), reduce Eq. (24) to

$$\gamma^2(\gamma-\delta)+1+q=0. \tag{25}$$

Equation (25) is essentially the same as Eq. (13.26) in Ref. [24] for the case in which the guiding magnetic field is absent. It is clear from Eq. (25) that the transverse interaction enhances the wave growth by a factor of $1+q$. Introducing a new gain parameter $D^3=C^3(1+q)$, one can rewrite Eq. (25) in the standard form [24],

$$\gamma^2(\gamma-\delta)+1=0, \tag{26}$$

where γ and δ are normalized to D instead of C, so the real growth rate γ now scales proportionally to D. Note that, as follows from Eq. (25), in the absence of a guiding magnetic field, the devices can operate not only in TM but also in TE modes, as was demonstrated experimentally by Goebel *et al.* [12].

B. Large-signal operation

The wave amplification and saturation in a TWT free from a guiding magnetic field is illustrated by Fig. 1, which shows the results of the study of Eqs. (19)–(21) for the case of $\alpha_0=0.1$, $\rho_0=3$ and different values of Δ. It was assumed that the wall radius corresponds to $\rho_w=4$. The thin line in Fig. 1 shows, for the sake of comparison, the same case, $\Delta=1.5$, when the radial motion of electrons is excluded from consideration. So, when $\rho=$ const, the wave grows slower [in

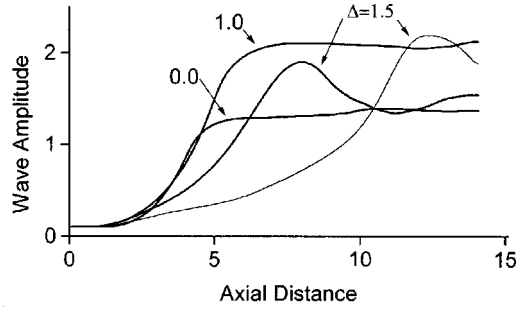

FIG. 1. Wave amplitude as the function of the normalized axial coordinate for different detunings of the Cherenkov synchronism Δ (a thin line shows the same dependence for the case when the radial motion of electrons is canceled).

accordance with Eq. (25)]; however, when ρ varies, the maximum amplitude is smaller because of the electrons intercepting with the wall.

The latter process is illustrated by Fig. 2, which shows the trajectories of electrons with different entrance phases for the cases presented in Fig. 1. When the mismatch Δ is in the range of 0 [Fig. 2(a)] to 1.0 [Fig. 2(b)], the beam interception starts just when the wave amplitude reaches its maximum. Then the process of interception stabilizes the wave amplitude. In the case of $\Delta=1.5$ shown in Fig. 2(c), the electron bunch is formed in such a phase that the radial electric field first protects particles from interception, and the beam starts to spread radially outward only after the wave amplitude passes the first maximum.

The effect of the axial and radial forces on electrons is illustrated by Fig. 3, which shows the location of electrons in

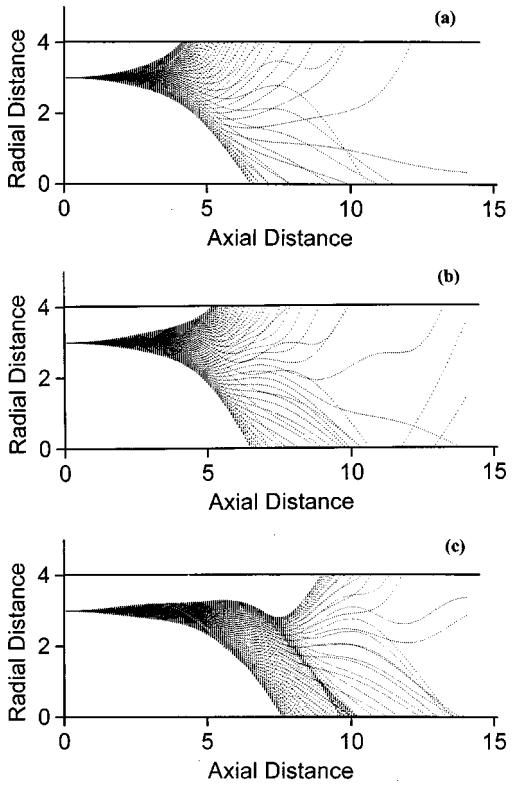

FIG. 2. Radial expansion of the beam for several detunings: (a) $\Delta=0$, (b) $\Delta=1.0$, and (c) $\Delta=1.5$.

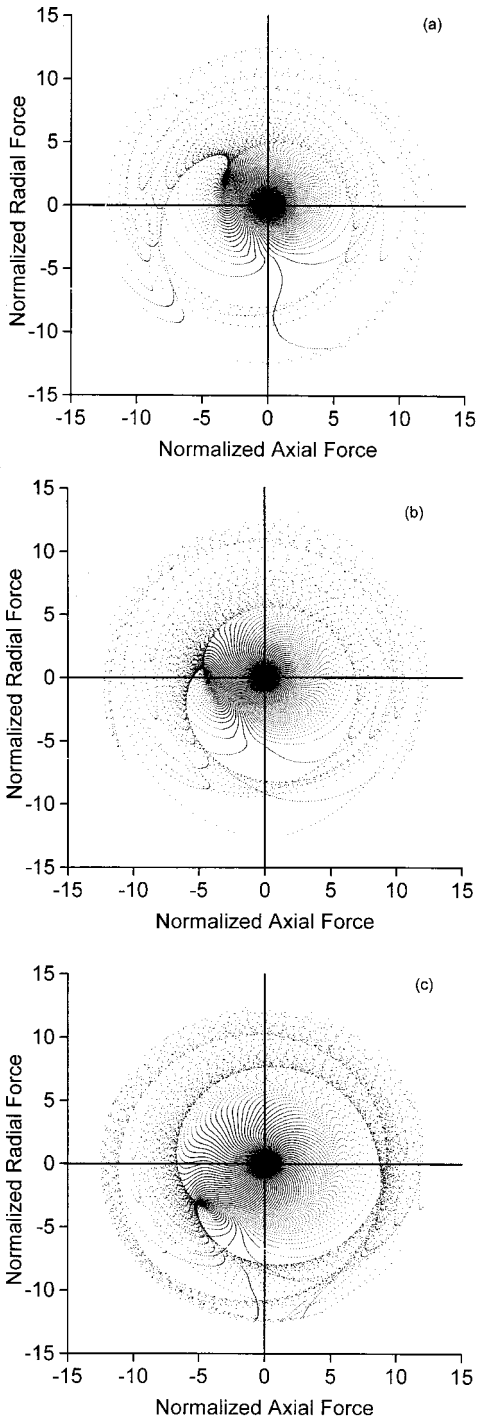

FIG. 3. Location of electrons in the plane $y=\zeta\sin(\theta+\phi)$ vs $x=\zeta\cos(\theta+\phi)$, illustrating the effect of the axial (proportional to x) and radial (proportional to y) forces on electrons. Each cross section corresponds to a circle with a radius $\zeta=\sqrt{x^2+y^2}$.

the plane $y=\zeta\sin(\theta+\phi)$ versus $x=\zeta\cos(\theta+\phi)$. Here, ϕ is the phase of the complex amplitude, $\alpha=|\alpha|e^{i\phi}$, so the vertical axis corresponds to the force causing the radial displacement [see Eq. (20)], and the horizontal axis shows the force causing the electron axial bunching [see Eq. (19)]. For characterizing the electron location in different cross sections, the variables x and y are proportional to the normalized axial distance ζ. So, to analyze the location of particles in a given cross section, $\zeta=$ const, one should consider a circle of

given radius $\zeta=\sqrt{x^2+y^2}$ in this plane. Then the area with the largest density of particles shows where the bunch is located, and the azimuthal position of this bunch shows the effect of the radial and axial components of the force acting on it. As follows from Figs. 3(a) and 3(b), in the range of Δ's from 0 to 1.0, the bunch is formed in such a phase that the radial force causes a radial expansion of the beam, while in the case of $\Delta=1.5$ shown in Fig. 3(c), the bunch is formed in a phase that corresponds to the focusing of electrons by the radial field.

V. EFFECT OF IONS

In such microwave sources as PASOTRON's, the interaction region is initially filled with a neutral gas (helium at a pressure $\sim 10^{-5}$ torr and/or xenon at a pressure $\sim 10^{-4}$ torr). This low pressure gas is ionized by beam electrons that, as shown in Ref. [25], are initially spread out due to the beam's electric self-field. Then the appearance of ions causes beam focusing and, simultaneously, the plasma electrons due to the beam's self-field reach the walls. (Note that, in principle, plasma electrons propagating in the interaction region of a MW-class microwave source acquire enough oscillatory energy for further ionization of such gases as He, which was used in several experiments [9,11,12].)

Typically, it takes about 5–6 μ sec [25] for the beam to start propagating through an SWS in a quasistationary regime of ion focusing. In this regime, the ratio of the ion density to the beam density, $f=n_i/n_b$, is close to $1/\gamma_0^2$ [26].

Since the ion density in the beam region is smaller than the beam density, the beam space charge causes the formation of an ion layer around the beam. When $n_i=n_b/\gamma_0^2$, the radius of this ion layer, which neutralizes the beam space charge, relates to the beam radius as $r_{i,\mathrm{out}}=\gamma_0 r_b$. So, in the beam region, there are beam electrons and ions with $n_i=n_b/\gamma_0^2$, then, at $r_b<r<r_{i,\mathrm{out}}$, there is an ion region that creates a potential well for beam electrons which can move radially under the action of the radial electric field of the wave; finally, at $r>r_{i,\mathrm{out}}$ there is a region of quasineutral plasma.

The thickness of the ion layer, d_i, as follows from the beam charge compensation by ions, is equal to

$$d_i=\frac{1}{e2\pi r_i v_0 k}. \tag{27}$$

Here k is the coefficient for the dependence of the ion density on the beam current, $n_i=kI_b$; this coefficient depends on the ionization cross section, the geometry of the interaction region, and other factors.

Assuming that the thickness of ion layer, d_i, is much smaller than its inner radius, $r_{i,\mathrm{in}}$, one can readily find that, to be in equilibrium, the electrons should have a radius r_{b0} that corresponds to the bottom of the potential well created by the ions:

$$r_{b0}=r_i+\frac{d_i}{2\gamma_0^2}. \tag{28}$$

For low-voltage operation, this means a radius that corresponds to the exact middle of the ion layer.

Taking into account the beam self-fields and the effect of ions, one can rewrite Eq. (20) for electron radial motion as

$$\frac{d^2\rho}{d\zeta^2}=\hat{I}_1(\rho)\mathrm{Im}(\alpha e^{i\theta})-\Lambda\frac{\rho_0}{\rho}\times\left[\frac{1}{\gamma_0^2}-2\begin{cases}0, & \rho<\rho_i\\ (\rho-\rho_i)/\delta_i\rho_i, & \rho_i\leqslant\rho\leqslant\rho_i(1+\delta_i)\\ 1, & \rho>\rho_i(1+\delta_i)\end{cases}\right]. \tag{29}$$

Here, the first term $(1/\gamma_0^2)$ in square brackets originates from the superposition of the electric and magnetic self-fields of the beam acting upon electrons (see, e.g., Ref. [26]); $\delta_i=d_i/r_i$ is the relative thickness of the ion layer, and

$$\Lambda=\frac{eI_b}{m_0c^3}\frac{\gamma_0^2}{(\gamma_0^2-1)^2}\frac{1}{C^2}\frac{\lambda}{2\pi r_{b0}}. \tag{30}$$

Since the Pierce gain parameter C is proportional to $I_b^{1/3}$, from the definition of Λ it follows that $\Lambda\sim I_b^{1/3}$; i.e., at low currents ($[I_b(kA)/17]^{1/3}\ll 1$), the effect of this additional term in Eq. (29) is small. Also note that as the initial beam radius becomes smaller, the radial electric field decreases while the current density, which determines the parameter Λ, increases. Therefore, the performance of the device with a given beam current may strongly depend on the initial beam position.

Since the radial electric field of the wave may play a defocusing role at certain phases θ, while the presence of ions always plays a focusing role, it makes sense to estimate the ion density required for the beam focusing. As follows from Eqs. (4) and (5), the radial force of the wave can be determined as $F_r\simeq A_s m_0\omega^2 r/2\gamma_0(\gamma_0^2-1)$. At the same time the focusing force caused by ions for electrons with $r=r_i$ is equal to $F_f=-2\pi e^2 n_i r/\gamma_0$. Correspondingly, the condition $|F_f|>F_r$ can be written as

$$\frac{\Omega_i^2}{\omega^2}>\frac{A_s}{\gamma_0^2-1}, \tag{31}$$

where $\Omega_i^2=4\pi e^2 n_i/m_0$ (here m_0 is the electron mass). Equation (31) shows that, to provide the same focusing effect at different power levels, the ion density should scale proportionally to the wave amplitude. Since the ion density is proportional to the beam current, which ionizes an initially neutral gas, it implies for the radiated power ($P\sim A_s^2$), a dependence on the beam current, $P\sim I_b^2$.

A. Traveling-wave tubes

The presence of ions may cause different effects in the operation of such a plasma-filled TWT, depending on the initial beam radius r_{b0}. Some of these effects are illustrated in Fig. 4, which shows the axial profile of the wave envelope for three values of r_{b0}. At small r_{b0}'s electrons have a large initial clearance, so they move radially toward the wall where the coupling impedance becomes larger, and reach the wall only after passing through the second maximum of the wave. (This second maximum is larger than the first simply

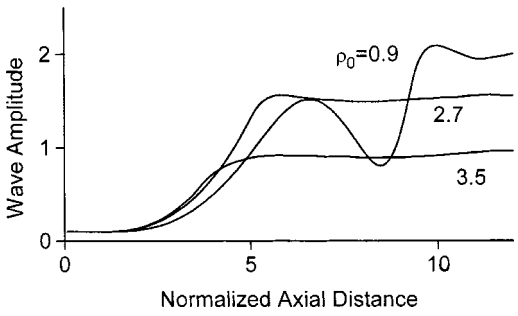

FIG. 4. Axial dependence of the wave amplitude for $\Delta=0$, $\alpha_0=0.1$, $\rho_w=4$, $\Lambda=0.3$, and different initial beam radii.

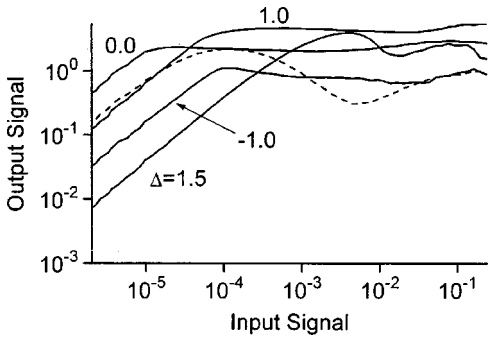

FIG. 6. Normalized output power vs input power for several values of the mismatch of Cherenkov synchronism Δ.

because of the difference in coupling impedances.) At moderate r_{b0}'s (the case of $\rho_0=2.7$ is shown in Fig. 4), electrons reach the wall only in the cross section where the wave amplitude has its first maximum. Finally, at large r_{b0}'s ($\rho_0=3.5$ in Fig. 4), electrons hit the wall before the first maximum of the wave and this interception causes the wave saturation. This effect is also illustrated by 5(a)–5(d). Figures 5(a) and 5(b) show the electron motion and the axial distribution of the wave envelope for a small initial radius, ($\rho_0=0.7$): (a) corresponds to the absence of ions, and (b) to the case when $\Lambda=0.3$. So, in the former case, the electrons reach the wall when the wave amplitude is at its maximum, while in the latter case the electrons are confined in the potential well. In contrast, when the initial radius of the electrons is large [$\rho_0=3$ in Figs. 5(c) and 5(d)], the electron trajectories are very much the same in the cases when $\Lambda=0$ [Figs. 5(c)] and $\Lambda=0.3$ [Fig. 5(d)].

The above-mentioned saturation of the wave amplitude by the beam interception with the walls may lead to a quite specific dependence of the output signal $|\alpha(\zeta_{\text{out}})|^2$ on the input signal $|\alpha_0|^2$. In this case, at low levels of P_{in}, the output power grows linearly with P_{in}, while, starting from a certain level of P_{in} the output power remains constant. As shown in Fig. 6, for the device under study, this dependence exists in a wide range of detunings, Δ (from -1.0 to $+1.0$); i.e., such performance, which is of interest for digital communication systems [27], can be realized in a large bandwidth.

B. Backward-wave oscillators

It seems expedient to expect that the effect of the radial electric field on the operation of BWO's is stronger than in TWT's because in BWO's the wave amplitude is maximum near the electron entrance. Correspondingly, during their passage through the interaction space the electrons can be strongly deflected radially.

The operation of BWO's strongly depends on the reflection coefficient of waves from the exit [22]. When the reflection coefficient is close to 100%, the axial structure of the field excited by the beam is fixed. Correspondingly, the operation of such a BWO can be described by Eqs. (19) and

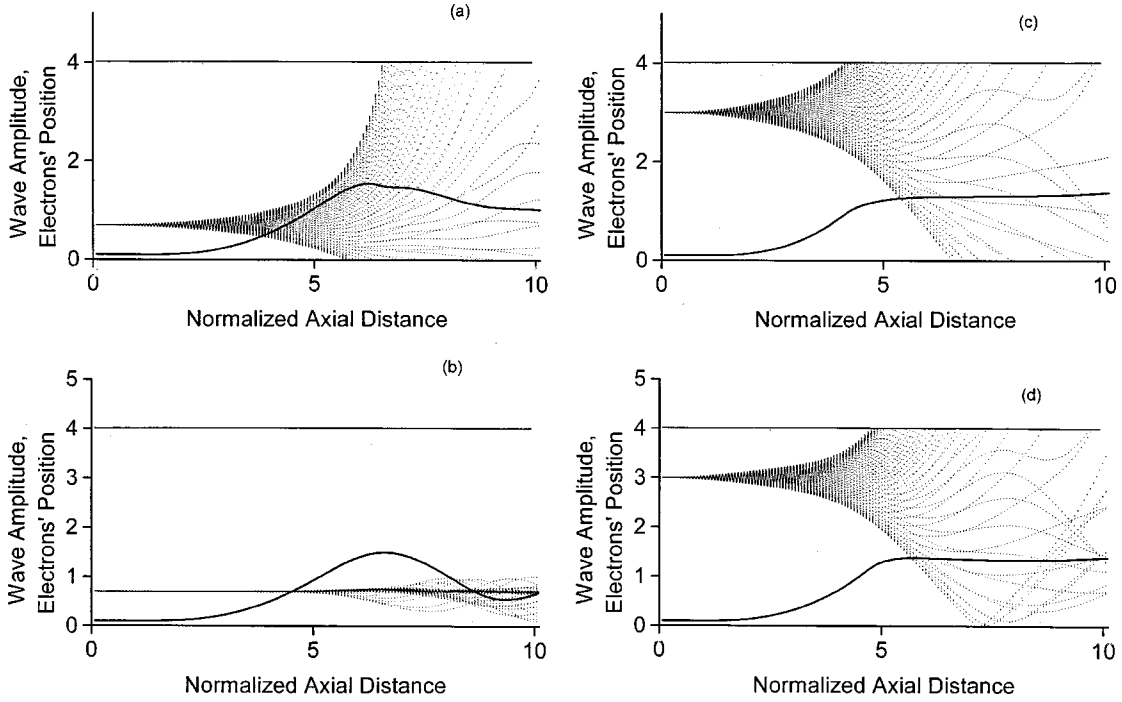

FIG. 5. The axial dependence of the wave amplitude and electron trajectories for $\Delta=0$, $\alpha_0=0.1$, and $\rho_w=4$ and (a) $\Lambda=0$, $\rho_0=0.7$; (b) $\Lambda=0.3$, $\rho_0=0.7$; (c) $\Lambda=3$; and (d) $\Lambda=0.3$, $\rho_0=3$.

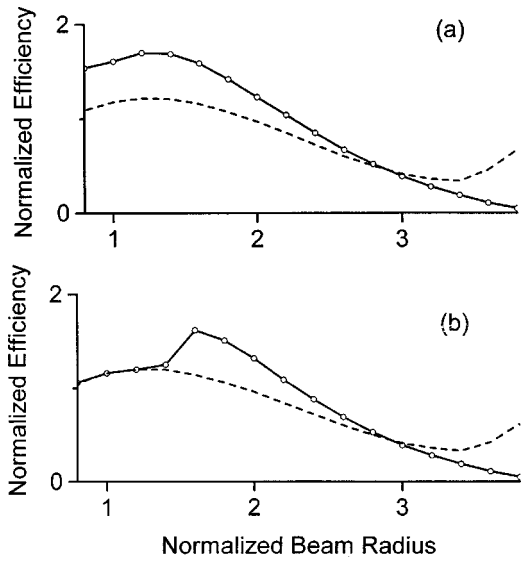

FIG. 7. Normalized efficiency as the function of the initial beam radius in the vacuum device (a) and in the presence of ions with $\Lambda=0.3$ (b). Solid and dashed lines correspond, respectively, to the cases when the radial electric field of the wave is taken into account and ignored.

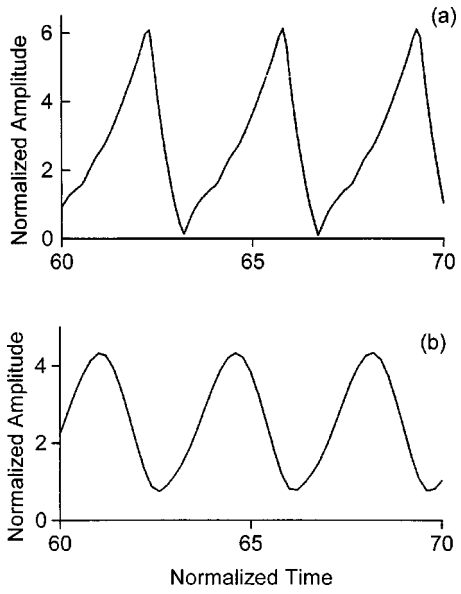

FIG. 8. Temporal evolution of the wave amplitude at the entrance to a plasma-filled BWO for $\Lambda=0.6$ (a) and 1.6 (b).

(29) for electron motion, and the standard equation for the excitation of a cavity mode with a fixed spatial structure (see, e.g., Eq. (21) in Ref. [28]).

Some results of the study of such devices are presented in Figs. 7(a) and 7(b). In Fig. 7(a), the normalized efficiency determined by Eq. (22) is shown for the case $\Lambda=0$. Here the dashed line shows the case in which the radial motion of electrons is neglected, while the solid line shows the case in which this motion is taken into account. As follows from the comparison of these lines, at small initial radii of the beam, the radial motion enhances the efficiency since particles move to the region of stronger interaction with the wave. However, at large radii ($\rho_0>3$ for the system with the normalized wall radius $\rho_w=4$), electrons reach the wall very quickly so the efficiency decreases. In Fig. 7(b), the same curves are shown for the case of nonzero Λ. [The parameter Λ, determined by Eq. (30), is equal to 0.3 for $\rho_0=2$.] As follows from Fig. 7(b), at small initial radii ($\rho_0<1.4$), the effect of the radial electric field is negligibly small because Λ is large, so electrons are trapped in the potential well. However, at large initial radii (when $1.4<\rho_0<3$), the effect of this well is not as strong. Therefore, electrons can move through the potential barrier created by ions toward the wall, and this causes a noticeable increase in the efficiency.

We have also studied nonstationary processes in BWO's with a low Q SWS. To do this, we analyzed Eqs. (19) and (29) for electron motion and a properly normalized Eq. (15) for spatiotemporal evolution of the wave envelope. We analyzed a system with a relatively low reflection coefficient $R=0.7$, a normalized length $\zeta_{\text{out}}=2.5$, an initial beam radius $\rho_0=1.25$, a wall radius $\rho_w=4.0$, and various values of the parameter Λ. It was found that at small enough Λ's, the BWO operates in the steady-state regime. When Λ exceeds the threshold value (which is a little smaller than 0.6), a strong automodulation appears. In the case of $\Lambda=0.6$ shown in Fig. 8(a), the system exhibits some kind of strong relaxation oscillations. At larger Λ's, the automodulation becomes smaller, and it looks like a quasiharmonic automodulation, as shown in Fig. 8(b) for $\Lambda=1.6$. Corresponding spectra are shown in Fig. 9, from which it follows that, in the case of relaxation oscillations, the spectrum is much wider. Note that a further increase in Λ makes the focusing effect of ions even stronger. This freezes the radial motion of electrons, which leads to the restoration of stationary oscillations at $\Lambda>2.0$. Let us emphasize that the automodulation described above appears due to the radial motion of electrons. Certainly, such an automodulation does not exist in systems with a strong guiding magnetic field.

Some examples of the correspondence of the radial motion of electrons to the wave envelope profile, which is vari-

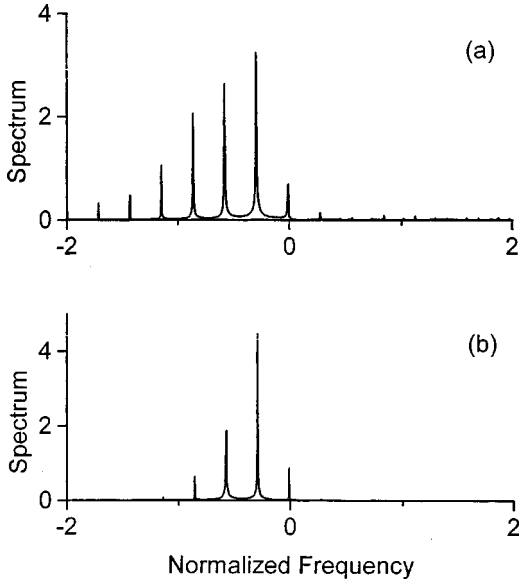

FIG. 9. Corresponding spectra of radiation for the cases of relaxation (a) and quasiharmonic (b) automodulation.

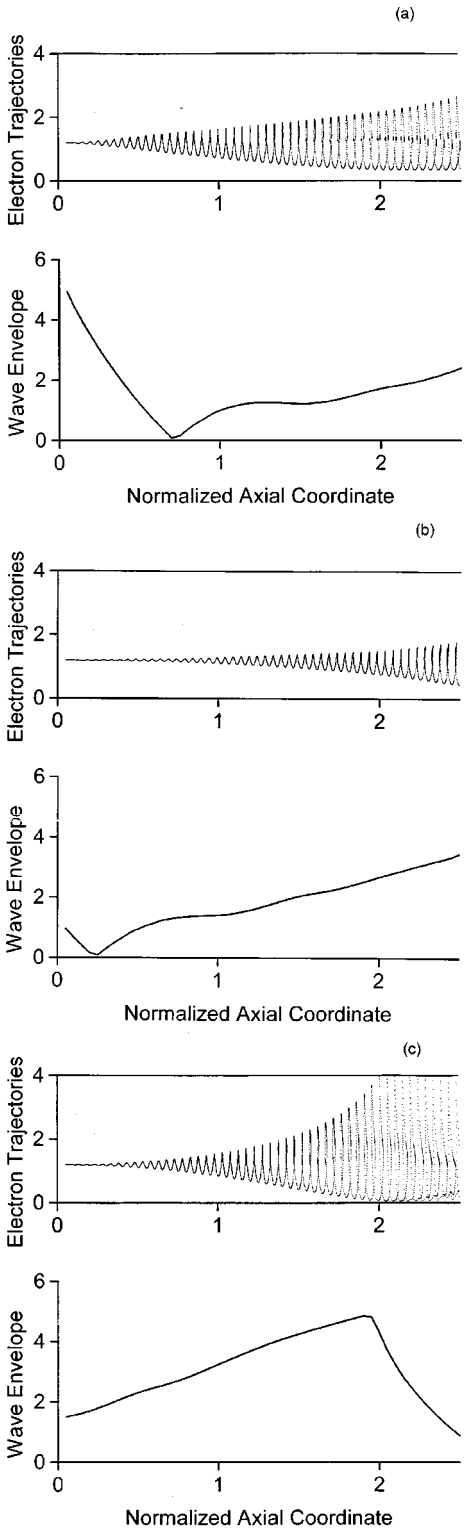

FIG. 10. Axial structure of the wave envelope and corresponding trajectories of electrons in plasma-filled BWO's operating in nonstationary regimes.

able in nonstationary regimes shown in Fig. 10. As seen in this figure, the beam interception by the wall again plays the role of the triggering mechanism, restricting the increase of the wave amplitude; as shown in Fig. 10(c), when this interception begins, the wave amplitude drastically decreases.

VI. SUMMARY

We have attempted to analyze the most important physical issues in the operation of Cherenkov microwave sources, in which the role of the focusing force required for the beam transport is played by ions instead of the external magnetic field. Due to the absence of a guiding magnetic field, the electrons can move radially, and this radial motion seems to be a very important feature of such devices for a number of reasons. First, the influence of the transverse electric field upon electrons moving radially may contribute to the energy exchange between electrons and the wave, and thus enhance the efficiency. In the framework of the small-signal theory, this increases the wave increment. In general, this effect makes the operation of Cherenkov sources in nonsymmetric transverse-electric modes possible. It also explains the experimentally observed operation of PASOTRON's in the $TE_{1,1}$ wave [9]. (Recall that the linear theory of transverse-field TWT's was developed by Pierce [24].) Second, a certain radial shift of electrons toward the wall due to the radial electric field of the wave is very beneficial, since it increases the beam coupling to a synchronous slow wave whose field is localized near the wall. This allows one not only to increase the efficiency, which is proportional to the Pierce gain parameter (which, in its turn, increases with the coupling impedance), but also to shorten the interaction space, which makes a device more compact. Note that a radial shift of electrons toward the wall can also be realized in the presence of an external magnetic field decreasing along the axis; however, this sort of operation does not allow one to explore the mechanism of transverse interaction discussed above. Recall that the fact of whether the radial electric field of the wave plays a focusing or defocusing role depends on the mismatch of the Cherenkov synchronism Δ, which, in turn, depends on the voltage. So the operation of such devices can be rather sensitive to even small variations in voltage.

Another interesting issue, which was analyzed above in a ''zero-order'' approximation, is the formation of a potential well due to the presence of ions around the beam with partially compensated space charge forces, and the effect of this well on the operation of devices. Although details of the formation of the ion channel were not analyzed above, one should expect that the depth of the potential well should be on the order of the potential of the Coulomb field produced by the beam. (In the case when the ion density increases, this should attract plasma electrons to ions, which will compensate for the excess of ions.) For electron beams of about 1-cm radius and ~100-A current, the Coulomb field has a potential on the order of several kV. This means that electrons can be untrapped from such a potential well by a wave with an electrical radial field strength on the order of kV/cm. For a slow-wave structure with a transverse size of a few cm, this corresponds to a microwave power at the MW level. When the generated power is at or above this level, we should not expect any significant effect of the structure of the ion channel on the performance of the device. So all our results of the analysis of stationary and nonstationary processes in slow-wave devices with ion-focused electron beams should be relevant to high-power experiments with plasma-filled devices. Recall that among these results are (a) a strong dependence of the efficiency on the initial position

of the beam, (b) a quite specific dependence of the output power on the input power in TWT's, where the saturation of the output power occurs due to the beam interception with the wall; (c) a competition between the focusing role of the potential well created by ions and the defocusing role of the radial electric field of the wave; and (d) a specific mechanism of automodulation in BWO's with relatively small end reflections in which the beam interception by the wall plays a triggering role. Certainly, to make a comparison of theoretical results with the available experimental data, a much more detailed numerical analysis should be done. Also, such issues as the stability of intense electron beams used in PASOTRON's, and the possibility of controlling the PASOTRON operation by applying a small external magnetic field, should be analyzed.

ACKNOWLEDGMENT

This work was sponsored by the Air Force Office of Scientific Research.

[1] S. J. Smith and E. M. Purcell, Phys. Rev. **92**, 1069 (1953).
[2] M. Chodorow and C. Susskind, *Fundamental of Microwave Electronics* (McGraw-Hill, New York, 1964).
[3] A. S. Gilmour, Jr., *Principles of Traveling Wave Tubes*, (Artech, Boston, 1994).
[4] N. F. Kovalev, M. I. Petelin, M. D. Raizer, A. V. Smorgonskii, and L. E. Tsopp, Pis'ma Zh. Eksp. Teor. Fiz. **18**, 138 (1973) JETP Lett. **18**, 81 (1973).
[5] Y. Carmel, J. Ivers, R. E. Kribel, and J. Nation, Phys. Rev. Lett. **33**, 1278 (1974).
[6] S. D. Korovin, S. D. Polevin, A. M. Roitman, and V. V. Rostov, Pis'ma Zh. Tekh. Fiz. **18**, 265 (1992) [Sov. Tech. Phys. Lett. **18**, 265 (1992)].
[7] S. D. Korovin, S. D. Polevin, A. M. Roitman, and V. V. Rostov, Pis'ma Zh. Tekh. Fiz. **20**, 5 (1994) [Tech. Phys. Lett. **20**, 5 (1994)].
[8] P. Wang, Z. Xu, D. Flechtner, Cz. Golkowski, Y. Hayashi, J. D. Ivers, J. A. Nation, S. Banna, and L. Schachter, *Proceedings of the Particle Accelerator Conference, March 1999* (IEEE, New York, 1999), Vol. 5, pp. 3600–3602.
[9] D. M. Goebel, J. M. Butler, R. W. Schumacher, J. Santoru, and R. L. Eisenhart, IEEE-PS **22**, 547 (1994).
[10] W. H. Benneth, Phys. Rev. **45**, 890 (1934).
[11] D. M. Goebel, IEEE Trans. Plasma Sci. **26**, 263 (1998).
[12] D. M. Goebel, R. W. Schumacher, and R. L. Eisenhart, IEEE Trans Plasma Sci. **26**, 354 (1998).
[13] F. J. Agee, IEEE Trans. Plasma Sci. **26**, 235 (1998).
[14] J. Benford and G. Benford, IEEE Trans. Plasma Sci. **25**, 311 (1997).
[15] N. F. Kovalev, Elektron. Tekh., Ser. 1, Elektron. SVCh. **3**, 102 (1978).
[16] J. A. Swegle, Phys. Fluids **30**, 1201 (1987).
[17] N. F. Kovalev, V. E. Nechaev, M. I. Petelin, and N. I. Zaytsev, IEEE Trans. Plasma Sci. **26**, 246 (1998).
[18] G. S. Nusinovich, Y. Carmel, T. M. Antonsen, Jr., D. M. Goebel, and J. Santoru, IEEE Trans. Plasma Sci. **26**, 628 (1998).
[19] L. A. Weinstein, Radiotekh. Elektron. (Moscow) **2**, 883 (1957).
[20] N. M. Kroll, in *Physics of Quantum Electronics*, edited by S. F. Jacobs, M. Sargent III, and M. O. Scully (Addison-Wesley, Reading, MA, 1978), Vol. 5, p. 115; see also V. L. Bratman, N. S. Ginzburg, and M. I. Petelin, Opt. Commun. **30**, 409 (1979); A. Gover and P. Sprangle, IEEE Trans. Quantum Electron. **17**, 1196 (1981).
[21] S. H. Gold and G. S. Nusinovich, Rev. Sci. Instrum. **68**, 3945 (1998).
[22] B. Levush, T. M. Antonsen, Jr., A. Bromborsky, W. R. Lou, and Y. Carmel, IEEE Trans. Plasma Sci. **30**, 263 (1992).
[23] J. E. Rowe, *Nonlinear Electron-Wave Interaction Phenomena*, (Academic, New York, 1965), p. 191.
[24] J. R. Pierce, *Traveling-Wave Tubes* (Van Nostrand, Toronto, 1950), p. 173.
[25] E. S. Ponti, D. M. Goebel, and R. L. Poeschel, in *Intense Microwave Pulses IV*, edited by H. E. Brandt (SPIE, Denver, 1996), Vol. 2843, p. 240.
[26] R. B. Miller, *An Introduction to the Physics of Intense Charged Particle Beams* (Plenum, New York, 1982), Chap. 4.
[27] B. Levush (private communication).
[28] G. S. Nusinovich and Yu. P. Bliokh, Phys. Plasmas **7**, 1294 (2000)